geosciences

MDPI

Article

Key Factors of Precipitation Stable Isotope Fractionation in Central-Eastern Africa and Central Mediterranean

Charles M. Balagizi [1,2,3,*] and Marcello Liotta [3]

[1] Geochemistry and Environmental Department, Goma Volcano Observatory, 142, Av. du Rond point, Goma, Democratic Republic of the Congo
[2] Department of Chemistry, Institut Supérieur Pédagogique de Bukavu, PO Box 854, Bukavu, Democratic Republic of the Congo
[3] Istituto Nazionale di Geofisica e Vulcanologia, Sezione di Palermo, Via Ugo La Malfa, 153, 90146 Palermo, Italy
* Correspondence: balagizi.charles@gmail.com; Tel.: +243975803568

Received: 31 May 2019; Accepted: 24 July 2019; Published: 31 July 2019

Abstract: The processes of isotope fractionation in the hydrological cycle naturally occur during vapor formation, vapor condensation, and moisture transportation. These processes are therefore dependent on local and regional surface and atmospheric physical features such as temperature, pressure, wind speed, and land morphology, and hence on the climate. Because of the strong influence of climate on the isotope fractionation, latitudinal and altitudinal effects on the $\delta^{18}O$ and $\delta^{2}H$ values of precipitation at a global scale are observed. In this study, we present and compare the processes governing precipitation isotope fractionation from two contrasting climatic regions: Virunga in Central-Eastern Africa and the Central Mediterranean (Stromboli and Sicily, Italy). While Virunga is a forested rainy tropical region located between Central and Eastern Africa, the Mediterranean region is characterized by a rainy mild winter and a dry hot summer. The reported $\delta^{18}O$ and $\delta^{2}H$ dataset are from precipitation collected on rain gauges sampled either on a monthly or an approximately bimonthly basis and published in previous papers. Both regions show clearly defined temporal and altitudinal variations of $\delta^{18}O$ and $\delta^{2}H$, depending on precipitation amounts. The Central Mediterranean shows a clear contribution of local vapor forming at the sea–air interface, and Virunga shows a contribution from both local and regional vapor. The vapor of Virunga is from two competing sources: the first is the continental recycled moisture from soil/plant evaporation that dominates during the rainy season, and the second is from the East African Great Lakes evaporation that dominates during the dry season.

Keywords: precipitation; stable isotope; isotope fractionation; tracing water cycle; Virunga; Central and Eastern Africa; Central Mediterranean

1. Introduction

Oxygen and hydrogen stable isotopes ($\delta^{18}O$ and $\delta^{2}H$) are among the tracers widely used to understand the processes involved in water circulation in the hydrological cycle. Besides the fact that oxygen and hydrogen isotopes are naturally occurring and quantitatively available, the changes in their concentration ratios are easily recorded during physical or chemical processes involving water, making them ideal to trace water mass movement [1–5]. The changes in the concentration ratios of isotopes during physical or chemical processes are referred to as isotopic fractionation. The nature of the processes that have occurred can then be determined from the observed differences in the isotopic compositions [1,4].

$\delta^{18}O$ and $\delta^{2}H$ fractionation naturally occurs throughout phase changes in the hydrological cycle, i.e., evaporation, condensation and diffusion. During vapor formation from surface waters—e.g., oceans, lakes, large rives, wetlands, etc.—the water molecules with lighter isotopes (i.e., ^{16}O and ^{1}H) evaporate first, leaving the evaporating source enriched with the heavier isotopes (i.e., ^{18}O and ^{2}H) [6–8]. As a consequence, the resulting precipitation is depleted in ^{18}O and ^{2}H relative to the residual evaporating source, which becomes enriched [6,9]. Conversely, during precipitation formation, molecules with heavier isotopes condense first, leaving the residual moisture cloud with depleted isotopes. The combined effects of evaporation, condensation and diffusion on stable isotope fractionation in the hydrological cycle lead to both latitudinal—and, thus, climatic—and altitudinal isotope effects [8,10–12]. Condensation and rainout over the continent are largely equilibrium-based fractionation processes, whereas evaporation largely undergoes kinetic or diffusion isotope fractionation, which are wind speed and temperature dependent. A close relationship between $\delta^{18}O$ and $\delta^{2}H$ in precipitation is observed globally and is defined by Dansgaard's equation $\delta^{2}H = s * \delta^{18}O + d$ [8] (where s indicates the slope, d indicates the intercept of the deuterium excess (d-excess), and the equation is known as the Global Meteoric Water Line (GMWL)).

The d-excess is strongly correlated with the physical conditions under which precipitation forms, e.g., air temperature and relative humidity (RH), wind speed and sea surface temperature, and therefore responds to environmental changes [13–16]. Thus, d-excess has been used in climatic studies to better understand and compare past and/to present precipitation formation processes (e.g., [17–21]). On the other hand, the seasonal weather variation (e.g., precipitation amount and temperature) in a given region leads to seasonal variations in ^{18}O and ^{2}H values. An altitudinal effect is similarly observed in both ^{8}O and ^{2}H values of precipitation at a continental scale, or in a region showing significant variation in elevation of the sampling locations. Hence, at a global scale, climate variation induces differences in stable isotope fractionation processes in precipitation, while at a regional scale, weather, topography and land-cover generally govern the fractionation. This study aims to characterize and compare the stable isotope fractionation of precipitation from two contrasting climatic regions: a continental tropical rainforest region in Central-Eastern Africa and a homogeneous climatic region with a local source of sea-derived vapor in the Central Mediterranean. This comparison brings insight into the ways in which climate features influence the stable isotope fractionation of oxygen and deuterium in precipitation. Climate features of tropical rainforest regions include a relatively high and nearly constant monthly mean air temperature and RH (high evaporation), a long rainy season with extreme events such as rainstorms, and a short dry season. The moisture is mainly from evaporating soil and surface waters, with an important input from plant transpiration. Conversely, the climate in the Mediterranean region is principally characterized by rainy, mild winters and dry, hot summers. These differences in climate and meteorological features yield differences in ^{18}O and ^{2}H fractionation in precipitation from both regions. Even though previous studies and sample collections were carried out in different time periods, the comparison of available datasets provides useful insights on how different climatic settings affect the isotope composition of precipitation. A detailed comparison is, thus, highlighted and discussed in the present study.

2. Material and Methods

2.1. Study Areas' Geographical, Hydrographical and Climatic Settings

The first set of rainwater samples are from the Virunga region, in the eastern Democratic Republic of the Congo, which is a mountainous region (altitudes up to 4508 m a.s.l) located in the western branch of the East African Rift (Figure 1). At a local scale, it experiences combined effects from the Virunga mountain chain and the equatorial dense forest, which induce a local mountainous micro-climate [22]. The Virunga mountain chain consists of eight major volcanoes, of which only Nyiragongo (3470 m a.s.l) and Nyamulagira (3058 m a.s.l) are presently active [23–28]. The significant variations in altitudes in Virunga, often abrupt, are recorded in the noticed difference between the mean annual precipitation in

the Virunga lowlands (found below 2000 m a.s.l.; 1300–1700 mm yr^{-1}) and highlands (> 2000 m; up to 2300 mm yr^{-1}) [29,30]. Virunga has a bimodal precipitation regime: a dry season (July to August) and a wet season (September to June); with a short dry-like period observed from mid-January to late-February. The mean monthly air temperature in the lowlands is ~20 °C with daily maxima of 32 °C, while in the highlands, the mean monthly temperature is ~10 °C with daily minima of 7 °C [29]. Hence, the dominant temperature fluctuation occurs in the daily temperatures rather than in monthly or yearly mean temperatures. The hydrography of Virunga consists of Lake Kivu (1460 m a.s.l.; evaporation rates ~1500 mm yr^{-1}), Lake Edward (912 m a.s.l.), several springs, and middle to large rivers (see compilation in [22,30]). At the regional scale, Virunga is located at the border between the Central and Eastern Africa regions, where a humid rainforest tropical climate predominates. The Virunga mountains influence the regional wind circulation, particularly those of the lower atmosphere. Virunga is part of the African Great Lake Region (Figure 1), where Lake Victoria, Lake Tanganyika, Lake Malawi, Lake Albert, etc., large rivers, and wetlands impact the East African regional climate and moisture production [30]. These lakes, large rivers and wetlands are subject to important evaporation. The region abounds in large dense forests that mainly consist of national parks. The majority of these tropical rain forests are wet and clouded all year long, and are, thus, important sources of moisture through evapotranspiration, principally during the rainy season.

The second set of samples was collected from Sicily and Stromboli islands in the Central Mediterranean. From a geological point of view, Sicily represents part of the south-verging branch of the Apenninic–Maghrebian orogenic belt made up of a pile of nappes derived from the deformation of different Meso-Cenozoic domains resulting from the collision of the African and Eurasian tectonic plates [31]. The climate is a typically Mediterranean one: characterized by hot summer droughts and winter rain in the mid-latitudes, north of the subtropical climate zone. In summer, the subtropical high-pressure cells drift toward the Northern Hemisphere (from May to August). This coincides with substantially higher temperatures than in winter and little rainfall [32,33]. During the winter, the high-pressure cells drift back toward the equator, and the weather is dominated by cyclonic storms [34]. At ground level, the mean monthly relative humidity is always higher than 70% and close to 80% during the rainy season. The Mediterranean Sea represents an important source of energy and moisture for cyclone development [33]. Several authors have provided detailed descriptions of climatic features and cyclogenesis in the Mediterranean, and have related them to orographic effects [35,36] and to large-scale circulation [37,38]. In addition, climate change is believed to be responsible for the increased intensity of cyclones over the Mediterranean Sea [39]. The hydrological cycle in the Mediterranean has been described by [40]. These authors have shown that evaporation from the Mediterranean Sea is greatest during the winter and in its eastern part. Climatic features and the soil types are responsible for the poor vegetation coverage of the studied area.

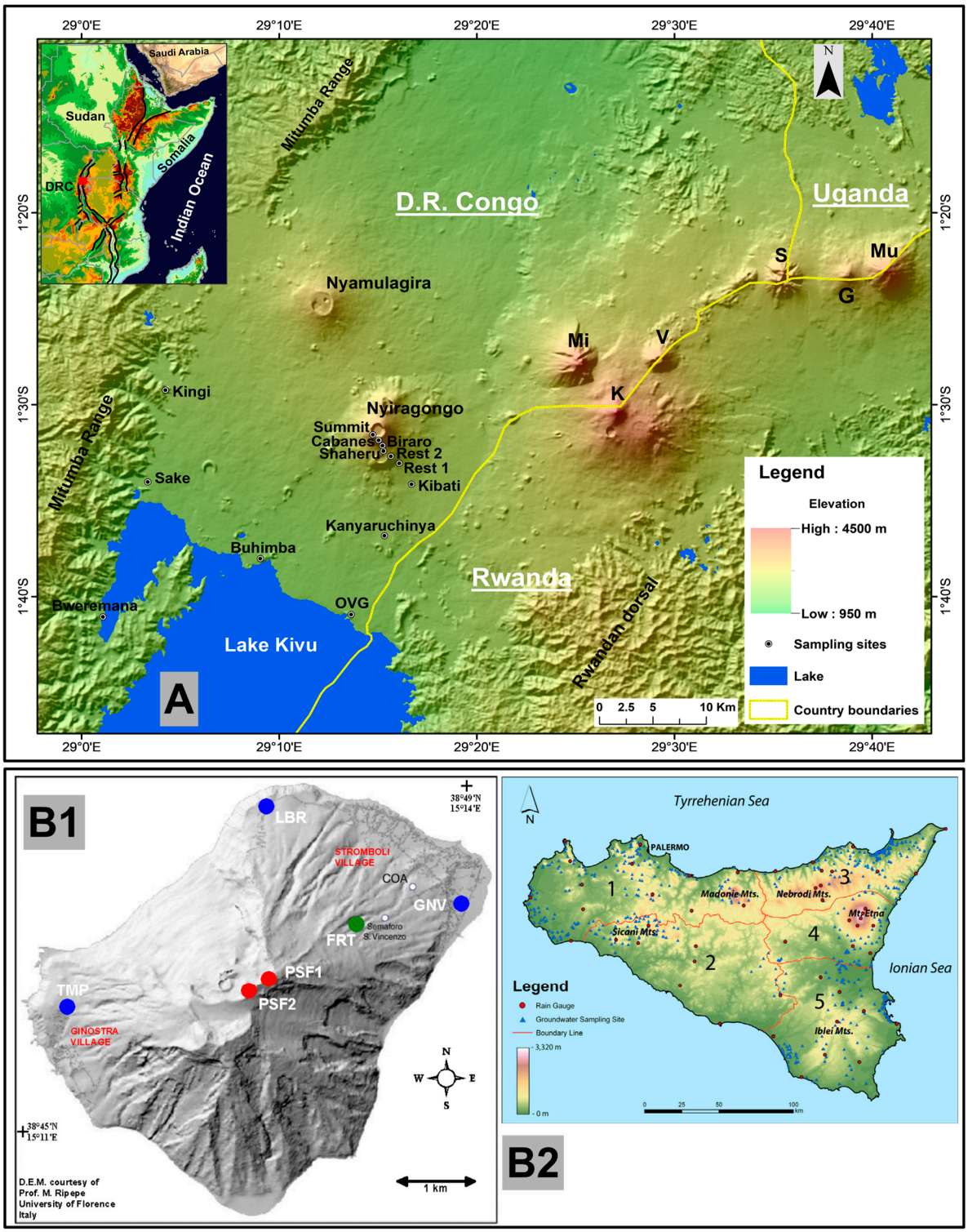

Figure 1. Topographic map of Virunga (**A**) located on the limit between Central and Eastern Africa, within the western branch of the East African Rift System (see insert map of **A**); Stromboli (**B1**) and Sicily (**B2**) (Italy) in the Central Mediterranean. In Virunga, the sampling sites are situated in the north basin of Lake Kivu and on Mt Nyiragongo (3470 m a.s.l.). On the map (**A**), Mt Nyamulagira (3058 m a.s.l), Mt Mikeno (Mi, 4437 m a.s.l), Mt Karisimbi (K, 4508 m a.s.l), Mt Visoke (V, 3911 m a.s.l), Mt Sabinyo (S, 3647 m a.s.l), Mt Gahinga (G, 3474 m a.s.l), and Mt Muhabura (Mu, 4127 m a.s.l) are also shown. The sampling sites were designed in order to capture any spatial and altitudinal variations of the stable isotope composition of oxygen and deuterium in precipitation.

2.2. Sampling and Analytical Techniques

Rain samples were collected from rain gauges that consisted of a plastic funnel fixed on a plastic container; the latter was filled with approximately 250 cm^3 of pure Vaseline oil to avoid evaporation. In Virunga, the samples were collected monthly from December 2013 to October 2015. After collecting the required aliquot for laboratory analysis and measuring the monthly precipitation amounts, the containers were washed with distilled water, and changed every 2–3 months during the study period. Water samples were filtered in the field through 0.45-mm-pore-size polysulfone syringe filters and stored at room temperature in 30-mL high-density polyethylene plastic bottles with double screwcaps. No additives were added to the samples. In the Mediterranean, rain samples were collected during different time periods. In Sicily, a rain gauge network was installed and sampled monthly in the period February 2002 to March 2003. Single rain events were also collected from one site of the network during the period October 2005 to September 2006. Rain samples at Stromboli Island, Italy, were collected between October 2003 and October 2005 on an approximately bimonthly basis. Additional rain samples were collected monthly in Sicily from May 2004 until June 2006, from a network of 50 rain gauges [32,33,41,42].

The majority of the samples from Virunga were analyzed for hydrogen and oxygen stable isotopes in the Isotope Hydrology Laboratory of the International Atomic Energy Agency (IAEA) in Vienna, Austria. The analyses were performed using an off-axis integrated cavity output laser spectroscopy (OA-ICOS), following the analytical procedure of [43]. Samples were first run in duplicate on a different day and instrument. Samples for which repeatability of the two runs was not within 2 times the typical uncertainty were repeated on a dual-inlet isotope ratio mass spectrometer (Isoprime DI 100) following equilibration with H_2 or CO_2 gases respectively [44]. A few of the samples from Virunga were analyzed at the Istituto Nazionale di Geofisica e Vulcanologia (INGV) in Palermo using Analytical Precision AP 2003 and Finnigan MAT Delta Plus spectrometers to analyze $\delta^{18}O$ and $\delta^{2}H$, respectively [30]. The majority of the samples from the Mediterranean was analyzed at the Istituto Nazionale di Geofisica e Vulcanologia (INGV) in Palermo. Details on the analytical methods are described in [32,33,41,42].

The oxygen and hydrogen isotopic compositions of a sample are reported as the deviation of the isotopic ratio of the sample relative to that of an established reference material (standard), and calculated as following:

$$\delta^{18}O = \frac{{}^{18}R_{sample} - {}^{18}R_{standard}}{{}^{18}R_{standard}} \text{ x } 10^3 \text{ (‰)}, \text{ and } \delta^{2}H = \frac{{}^{2}R_{sample} - {}^{2}R_{standard}}{{}^{2}R_{standard}} \text{ x } 10^3 \text{ (‰)}$$

where $\delta^{18}O$ and $\delta^{2}H$ represent, respectively, the oxygen and hydrogen isotope composition of the sample. R refers to the ratio between natural abundances of the rare to abundant isotopes of the element, which results in ${}^{18}R = {}^{18}O/{}^{16}O$ for oxygen and ${}^{2}R = {}^{2}H/{}^{1}H$ for hydrogen. Ocean water is the internationally established zero point of the delta notation for $\delta^{18}O$ and $\delta^{2}H$ of water [6,7], and is known as the Vienna-Standard Mean Ocean Water (V-SMOW). For both Virunga and Mediterranean, the d-excess was deduced from Dansgaard's equation [8], relating the $\delta^{18}O$ and $\delta^{2}H$ of water, by the relationship $d = \delta^{2}H\text{-}8\delta^{18}O$. The typical uncertainty is reported as the long-term standard deviation of a dedicated control sample and is 0.08‰ for $\delta^{18}O$ and 0.50‰ for $\delta^{2}H$.

3. Results and Discussion

3.1. General Variabilities

The isotopic composition of the precipitation of both regions has monthly values that are spread over a wide range (Table 1), particularly for $\delta^{2}H$ (Figure 2), with Virunga showing the higher $\delta^{18}O$ and $\delta^{2}H$ values and the Central Mediterranean showing the most negative (Figure 2A). Thus, Virunga monthly values span from −32.53 to 58.89‰ for $\delta^{2}H$ and −6.44 to 6.16‰ for $\delta^{18}O$ (N = 223), and for the Central Mediterranean, from −74.20 to 18.00‰ for $\delta^{2}H$ and −11.60 to 3.60‰ for ${}^{18}O$ (N = 1272)

(Table 1). As a general tendency for both regions, the higher δ values were obtained during the dry periods: the dry and warm season in Virunga and dry and hot summer months in the Central Mediterranean. These periods are characterized by very low precipitation, yielding the observed $\delta^{18}O$ and $\delta^{2}H$ enrichment. Furthermore, the most negative values were obtained during the heavy rainy season in Virunga and during the cold and wet winter period in the Central Mediterranean.

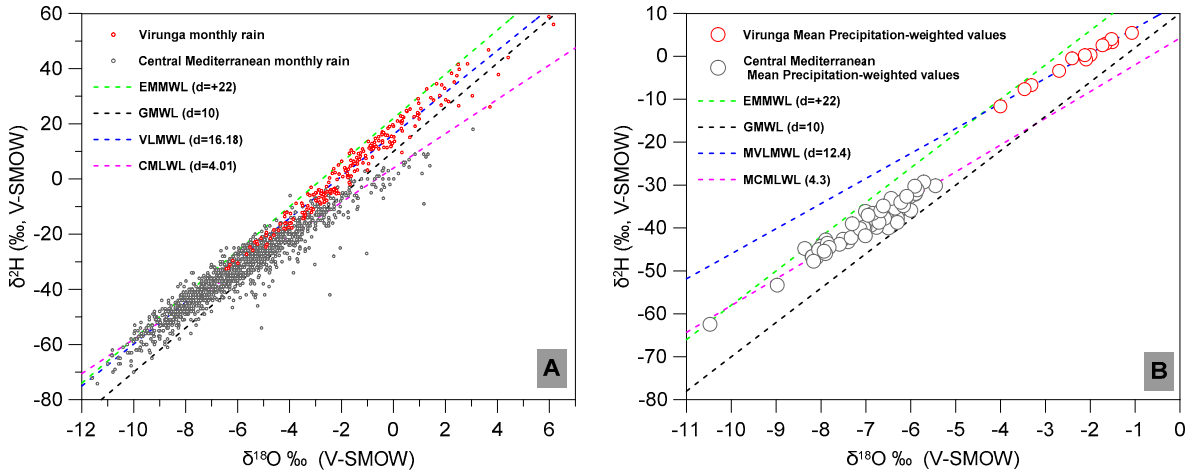

Figure 2. Relationship between $\delta^{2}H$ and $\delta^{18}O$ in monthly rainwater from the Virunga region, located on the limit between Central and Eastern Africa, within the western branch of the East African Rift System, and the Central Mediterranean (Stromboli and Sicily Islands, Italy). In (**A**) and (**B**), EMMWL refers to the Eastern Mediterranean Meteoric Water Line after Gat and Carmi [13], and GMWL to the Global Meteoric Water Line after Craig [6]. In (**A**) the Virunga Local Meteoric Water Line (VLMW), and the Central Mediterranean Local Meteoric Water Line (CMLWL) are plotted; both lines were obtained using monthly values. In (**B**), the Mean Virunga Local Meteoric Water Line (MVLMWL) and Mean Central Mediterranean Local Meteoric Water Line (CMLWL) are plotted, and both were obtained using mean precipitation-weighted values.

Strong positive correlations are observed between the $\delta^{18}O$ and $\delta^{2}H$ of precipitation when monthly values are used, and show Ordinary Least Squares Regression (OLSR) lines of $\delta^{2}H = 7.60\ \delta^{18}O + 16.18$ ($r^2 = 0.96$; $p < 0.0001$ and $N = 223$) for Virunga, and $\delta^{2}H = 6.21\ \delta^{18}O + 4.01$ ($r^2 = 0.91$; $p < 0.0001$ and $N = 1272$) for the Central Mediterranean. These lines are strongly influenced by extreme values that have higher $\delta^{18}O$ than that of their corresponding Local Meteoric Water Lines (LMWL) in particular, and than that of the GMWL in general (Figure 2A). In such circumstances, precipitation-weighted values are commonly recommended for the calculation of the LMWL. These extreme values are typically the result of extreme weather conditions (e.g., at the peak of the dry or wet periods, or during thunderstorms) or due to secondary processes that may affect raindrops during their fall and that modify the isotopic composition of the pristine rainwater. This point is further discussed in Section 3.4. Hence, the mean precipitation-weighted values for the Central Mediterranean vary from −62.45 to −29.28‰ for $\delta^{2}H$ and −10.47 to −5.45‰ for $\delta^{18}O$; and from −11.79 to 5.45‰ for $\delta^{2}H$ and from −4.00 to −1.07‰ for $\delta^{18}O$ in Virunga (Figure 2B). Thus, using the precipitation-weighted values, the equations for the LMWL are $\delta^{2}H = 5.84\ \delta^{18}O + 12.34$ ($r^2 = 0.99$; $p < 0.0001$; $N = 13$) for Virunga, and $\delta^{2}H = 6.23\ \delta^{18}O + 4.25$ ($r^2 = 0.93$; $p < 0.0001$; $N = 67$) for the Central Mediterranean. These equations are referred to as the Mean Local Meteoric Water Lines (MLMW), MVLMW for Virunga and MCMLWL for the Central Mediterranean (Figure 2B). The higher enrichment of Virunga precipitation clearly emerges when precipitation-weighted values are used (Figure 2B).

Table 1. Sampling sites elevation (meter, m), monthly min, average and max δ^2H, $\delta^{18}O$ and deuterium excess (per mil) of rainwater collected on a monthly basis in Central Mediterranean (Stromboli and Sicily, Italy) and in Central-Eastern Africa (at Mount Nyiragongo and the surroundings, Democratic Republic of the Congo).

Site Name	Elevation (m a.s.l.)	UTM Coordinates		Precipitation (mm/month)			δ^2H (‰)			$\delta^{18}O$ (‰)			d−excess (‰)			Number of Samples	Sapling Periode	Region
		Easting	Northing	Min	Average	Max	Min	Average	Max	Min	Average	Max	Min	Average	Max			
FRT	282	519804	4294449	2.829054	112.1399	219.959	−48	−30.5455	−3	−8.4	−5.90455	−2.15	11.6	16.69091	20.8	11	2003–2005	Stromboli (Italy), Central Mediterranean
GNV	5	520890	4294699	2.121791	107.099	234.1043	−49	−28.2727	−6	−7.9	−5.17273	−1.5	6	13.10909	16.6	11	2003–2005	Stromboli (Italy), Central Mediterranean
LBR	121	518743	4295681	3.88995	101.3573	196.2656	−46	−28.9091	−3	−7.9	−5.37273	−1.7	10.6	14.07273	19	11	2003–2005	Stromboli (Italy), Central Mediterranean
PSF 1	881	518695	4293865	66.48278	115.9677	211.4718	−48	−41.8333	−35	−8.7	−7.71667	−6.8	16	19.9	21.8	6	2003–2005	Stromboli (Italy), Central Mediterranean
PSF 2	900	518600	4293724	61.95629	126.2466	170.4505	−51	−44.1667	−34	−9.4	−8.26667	−6.8	20.2	21.96667	25.2	6	2003–2005	Stromboli (Italy), Central Mediterranean
TMP	130	516708	4293638	2.829054	66.90714	145.4134	−48	−28.1111	−8	−8	−5.24444	−2.2	9.4	13.84444	18	9	2003–2005	Stromboli (Italy), Central Mediterranean
S. Ninfa	470	313600	4182900	4.950845	53.44892	141.1698	−74.2	−30.6769	4.8	−11.4	−5.62308	1.4	−6.4	13.28571	23.2	14	2002–2003	Palermo (Italy), Central Mediterranean
Triscina	13	306000	4162000	8.487163	49.21039	154.4664	−67.7	−26	4.3	−10.1	−4.43571	0.6	−0.5	9.485714	16.1	14	2002–2003	Palermo (Italy), Central Mediterranean
Spagnuola	15	278200	4190500	2.829054	46.33587	118.3959	−62.1	−29.1846	−10.8	−9.4	−5.1	−2.8	4.1	11.61538	20.1	14	2002–2003	Palermo (Italy), Central Mediterranean
Trapati	12	283925	4212400	4.243582	38.46504	113.4451	−58	−29.2929	2.8	−8.7	−5.07857	−1.1	1.8	11.33571	20.1	14	2002–2003	Palermo (Italy), Central Mediterranean
Sparagio	1100	304900	4214550	4.243582	77.05132	193.2244	−63	−40.1429	−18.3	−10.2	−7.18571	−4.5	3	17.34286	24.1	14	2002–2003	Palermo (Italy), Central Mediterranean
Linici	980	312000	4208775	7.7799	76.11167	187.2834	−64.9	−42.6857	−23.5	−10.6	−7.47143	−5.4	7.8	17.08571	21.8	14	2002–2003	Palermo (Italy), Central Mediterranean
M. Grande	675	302050	4196300	5.941014	45.85089	135.7946	−72.2	−33.5929	−10.4	−11.6	−6.04286	−3.7	6	14.75	21.1	14	2002–2003	Palermo (Italy), Central Mediterranean
Calatafimi	400	312825	4197750	7.355541	57.77333	147.6766	−62.3	−33.8786	−16.4	−9.7	−5.99286	−4.1	5.9	14.06429	21	14	2002–2003	Palermo (Italy), Central Mediterranean
San Vito	15	301550	4228000	5.658109	43.93739	99.58271	−55	−33.0077	−4.9	−8.5	−5.45385	−2.2	1	10.62308	17.4	13	2002–2003	Palermo (Italy), Central Mediterranean
Scopello	60	312075	4213325	3.536318	59.97595	152.7689	−56.2	−32.1	−12.1	−8.5	−5.40833	−2.9	3.5	11.16667	18.4	12	2002–2003	Palermo (Italy), Central Mediterranean
INGV−Palermo	85	351950	4225700	10.32605	52.01108	127.0245	−60	−35.7154	−22.1	−8.8	−5.82308	−4	0.5	10.86923	18	13	2002–2003	Palermo (Italy), Central Mediterranean
Calatafimi	399	312795	4199058	8.346793	70.1107	239.369	−53	−31.2917	7	−9.16	−5.7314	0.6	2.2	14.55954	25.28	24	2004–2006	Palermo (Italy), Central Mediterranean
Santa Ninfa	470	313611	4182790	11.31768	72.60233	252.9503	−60	−30.5217	6	−9.95	−5.65887	0.46	−2.32	14.74921	24.6	22	2004–2006	Palermo (Italy), Central Mediterranean
Triscina	7	305439	4161952	1.414711	63.32438	263.7021	−63	−25.2273	−2	−9.37	−4.68546	−0.82592	4.451713	12.2564	19.44	22	2004–2006	Palermo (Italy), Central Mediterranean

Table 1. *Cont.*

Site Name	Elevation (m a.s.l.)	UTM Coordinates		Precipitation (mm/month)			δ^2H (‰)			$\delta^{18}O$ (‰)			d−excess (‰)			Number of Samples	Sapling Periode	Region
		Easting	Northing	Min	Average	Max	Min	Average	Max	Min	Average	Max	Min	Average	Max			
Spagnuola	5	278092	4190520	5.941785	55.0876	209.6601	−52	−26.5652	4	−8.43	−4.87347	−0.38	−6.76	12.42254	20.84	22	2004–2006	Palermo (Italy), Central Mediterranean
S. Vito	8	301597	4227994	6.507669	59.78921	200.1816	−53	−28.0417	3	−9.07	−5.13661	0.19	0.48	13.05121	20.56	22	2004–2006	Palermo (Italy), Central Mediterranean
M.te Sparagio	1113	304910	4214514	9.902974	66.57462	254.9309	−55	−29.1176	−2	−9.58	−5.64497	−0.75	4	16.04212	26.92	17	2004–2006	Palermo (Italy), Central Mediterranean
Palazzo Adriano	682	357534	4171989	3.395305	96.86052	374.3324	−60	−35.3333	0	−10.1	−6.14078	−1	−18.76	13.7929	22.8	24	2004–2006	Palermo (Italy), Central Mediterranean
Cefalù	200	417515	4207190	10.18592	77.16603	169.1994	−56	−35	−6	−9.3	−5.89516	−1.42	−13.36	12.16132	25.08	22	2004–2006	Palermo (Italy), Central Mediterranean
Milena	4444	388505	4148246	8.488264	63.20066	180.5171	−62	−33.6522	−10	−9.86	−5.86296	−1.37068	−0.44	13.25152	23.92	23	2004–2006	Palermo (Italy), Central Mediterranean
Lucca Sicula	531	350567	4160443	8.488264	93.67956	282.0933	−64	−34.0909	−10	−10.82	−6.17144	−2.65	1.04	15.28064	23.36	22	2004–2006	Palermo (Italy), Central Mediterranean
Biviere di Gela	15	441340	4098335	1.839124	51.41653	161.5098	−46	−24.7222	0	−7.38	−4.35556	0.01	−8.6	10.12222	19.6	18	2004–2006	Palermo (Italy), Central Mediterranean
Sant'Agata di Militello	18	467973	4213944	8.488264	64.76427	136.3781	−52	−31.1667	9	−8.63	−5.58133	1.16	−0.56	13.48394	21.56	24	2004–2006	Palermo (Italy), Central Mediterranean
Capo Calavà	236	494846	4224085	9.902974	83.32056	227.2025	−53	−33.5417	−12	−8.93	−5.98902	−2.3	−9.6	14.37051	26.44	24	2004–2006	Palermo (Italy), Central Mediterranean
S. Basilio	737	480777	4207739	34.236	108.2069	272.7562	−70	−41.6957	−23	−10.24	−7.16729	−3.85	−3.2	15.64269	22.48	24	2004–2006	Palermo (Italy), Central Mediterranean
S. Stefano di Camastra	102	442871	4208031	5.092958	64.78759	142.8858	−56	−31.6087	−2	−8.78	−5.6577	−0.13728	−0.90175	13.65287	21.08	24	2004–2006	Palermo (Italy), Central Mediterranean
M.te Soro	1853	473236	4198435	27.72833	133.9289	424.4132	−53	−41.6875	−16	−9.44	−7.66438	−3.96	15.16	19.6275	25.6	16	2004–2006	Palermo (Italy), Central Mediterranean
Alcara Li Fusi	391	473815	4208401	22.35243	97.96228	218.1484	−61	−36.6818	−9	−9.22	−6.56375	−2.93	8.6	15.82815	22.64	22	2004–2006	Palermo (Italy), Central Mediterranean
Cesarò	1112	474378	4188851	6.224727	69.09939	162.6917	−70	−40.0435	6	−11	−7.15508	0.39	2.88	17.19712	24.56	23	2004–2006	Palermo (Italy), Central Mediterranean
Novara di Sicilia	620	511434	4207778	4.244132	97.56787	336.7011	−61	−32.3333	−7	−9.75	−5.89777	−1.38842	3.705681	14.84885	24.12	24	2004–2006	Palermo (Italy), Central Mediterranean
Villa Miraglia	1525	469777	4196801	27.16244	169.9318	526.7516	−67	−43.88	−14	−10.52	−7.7932	−3.95	9.4	18.4656	27.36	23	2004–2006	Palermo (Italy), Central Mediterranean
Agrigento	297	378795	4132044	0	62.98157	242.7643	−58	−31.0952	−2	−9	−5.53821	−0.39844	1.187557	13.21044	21.96	23	2004–2006	Palermo (Italy), Central Mediterranean
INGV−Palermo	90	351989	4225546	6.507669	71.02462	159.2964	−57	−30.9565	8	−8.99	−5.44079	1.25	−2	12.56981	22.96	21	2004–2006	Palermo (Italy), Central Mediterranean

Table 1. *Cont.*

Site Name	Elevation (m a.s.l.)	UTM Coordinates		Precipitation (mm/month)			δ^2H (‰)			$\delta^{18}O$ (‰)			d−excess (‰)			Number of Samples	Sapling Periode	Region
		Easting	Northing	Min	Average	Max	Min	Average	Max	Min	Average	Max	Min	Average	Max			
Alì Terme	22	537113	4206322	2.829421	79.69536	219.846	−58	−28.5238	−7	−8.24	−5.01734	−0.39243	−3.86056	11.6149	19.96	21	2004–2006	Palermo (Italy), Central Mediterranean
Capo Peloro	21	557072	4235966	12.16651	60.17236	123.3628	−56	−29.0952	0	−8.6	−5.43903	−1.2337	9.16	14.41701	27.4	21	2004–2006	Palermo (Italy), Central Mediterranean
Termini Imerese	78	385118	4204971	3.253834	48.86141	121.3822	−66	−32.1429	0	−10.1	−5.61231	−0.18071	1.44569	12.75561	22.68	21	2004–2006	Palermo (Italy), Central Mediterranean
Cerasella	1175	421471	4185235	6.790611	61.26876	204.2842	−61	−37.0417	−14	−10.41	−6.85633	−3.28	10.04	17.809	24.2	24	2004–2006	Palermo (Italy), Central Mediterranean
Giacalone	402	346427	4212842	16.26917	119.6306	346.6041	−54	−34.381	9	−9.28	−6.0331	1.33	−1.64	13.88381	23.2	21	2004–2006	Palermo (Italy), Central Mediterranean
San Cono	485	446152	4125344	2.405008	73.8286	207.9625	−53	−31.7727	−11	−8.96	−6.05175	−2.54078	9.326234	16.64126	21.72	21	2004–2006	Palermo (Italy), Central Mediterranean
Ramacca	285	473149	4137764	3.112363	66.7676	307.1337	−69	−29.4286	3	−10.72	−5.66524	−0.43	6.44	15.89333	27.12	21	2004–2006	Palermo (Italy), Central Mediterranean
Alpe Cucco	950	360257	4192698	4.244132	86.2384	254.082	−62	−37.375	9	−9.91	−6.84458	0.83	2.36	17.38167	25.76	24	2004–2006	Palermo (Italy), Central Mediterranean
Assoro	389	449341	4161303	9.620032	77.37722	314.2072	−52	−30.8333	−14	−8.58	−5.68556	−2.49	2.92	14.65111	23.72	19	2004–2006	Palermo (Italy), Central Mediterranean
Ist. Radioastr. Noto	100	499100	4081357	2.970892	68.39483	228.9002	−48	−26	−11	−8.04	−5.01762	−2.68	6.36	14.14095	22.4	22	2004–2006	Palermo (Italy), Central Mediterranean
Alia	663	386487	4181833	9.33709	66.96297	159.2964	−62	−36.1429	0	−10.01	−6.52286	−0.41	3.28	16.04	23.84	21	2004–2006	Palermo (Italy), Central Mediterranean
Mussomeli	516	389373	4158418	6.790611	61.97719	158.7305	−59	−34.0909	−3	−9.84	−6.14227	−1.23	6.84	15.04727	23.84	21	2004–2006	Palermo (Italy), Central Mediterranean
Montagna del Vento	767	335693	4162523	4.244132	96.79315	280.9615	−63	−38.7778	−17	−10.25	−6.92389	−3	7	16.61333	22.2	18	2004–2006	Palermo (Italy), Central Mediterranean
Zafferana	715	508496	4171902	9.195619	136.6257	342.36	−51	−22.3158	0	−8.47	−4.69947	−1.66	3.64	15.28	24	19	2004–2006	Palermo (Italy), Central Mediterranean
Catania	200	506411	4153726	4.244132	73.00651	232.0125	−44	−25.5714	1	−7.25	−4.86929	−0.64	6	13.38286	20.8	14	2004–2006	Palermo (Italy), Central Mediterranean
Acqua Rossa	355	494777	4153726	4.951487	67.23917	249.1305	−47	−24.6875	−1	−7.79	−4.6875	−1.53	4.88	12.8125	19.6	16	2004–2006	Palermo (Italy), Central Mediterranean
Intraleo	1510	492349	4175399	0	92.30397	364.288	−65	−37.75	3	−10.52	−6.72	−0.41	1.88	16.01	22.96	19	2004–2006	Palermo (Italy), Central Mediterranean
Pizzi de Neri	2810	501512	4180052	4.951487	74.34304	392.5822	−59	−44.6923	−20	−9.71	−7.99692	−4.92	15.88	19.28308	25.08	13	2004–2006	Palermo (Italy), Central Mediterranean
Torre del Filosofo	2940	500106	4176734	13.43975	58.82838	198.0595	−64	−44.4167	−28	−10.84	−8.0725	−5.65	15.76	20.16333	23.6	12	2004–2006	Palermo (Italy), Central Mediterranean
Provenzana	1800	503224	4183140	3.536777	125.1274	396.119	−59	−38.1053	−4	−9.89	−6.74105	−2.61	12.12	15.82316	21.12	19	2004–2006	Palermo (Italy), Central Mediterranean

Table 1. *Cont.*

Site Name	Elevation (m a.s.l.)	UTM Coordinates		Precipitation (mm/month)			δ^2H (‰)			$\delta^{18}O$ (‰)			d−excess (‰)			Number of Samples	Sapling Periode	Region
		Easting	Northing	Min	Average	Max	Min	Average	Max	Min	Average	Max	Min	Average	Max			
Serra la Nave	1725	497906	4171934	7.780908	102.3147	361.1756	−63	−35.1905	−1	−10.08	−6.50714	−0.68	2.44	16.86667	28.16	20	2004–2006	Palermo (Italy), Central Mediterranean
Scordia	158	485847	4127555	6.224727	73.70642	337.4085	−57	−29.5455	−5	−9.22	−5.36727	−1.67	4	13.39273	23.36	22	2004–2006	Palermo (Italy), Central Mediterranean
Monte Lauro	980	484140	4108024	5.3759	89.63114	295.816	−56	−33.3913	−9	−9.43	−6.32565	−2.67	5.36	17.21391	27.6	23	2004–2006	Palermo (Italy), Central Mediterranean
Sortino	445	502202	4114957	9.620032	91.96293	381.9719	−67	−28.381	−6	−10.58	−5.57095	−1.98	6.4	16.18667	25.84	21	2004–2006	Palermo (Italy), Central Mediterranean
Ragusa	535	475984	4086105	6.507669	69.10524	227.344	−50	−32.35	−16	−8.79	−6.051	−2.5	4	16.058	25.08	20	2004–2006	Palermo (Italy), Central Mediterranean
Marina di Ragusa	5	460317	4071408	6.224727	68.12303	251.8185	−45	−29.0714	−13	−7.18	−5.31643	−2.34	2.72	13.46	21.28	14	2004–2006	Palermo (Italy), Central Mediterranean
Siracusa	15	524219	4106403	5.800313	66.54641	257.4773	−42	−28.0588	−6	−7.12	−5.20059	−1.83	−22.4	13.54588	21.72	17	2004–2006	Palermo (Italy), Central Mediterranean
Licata	52	405442	4106611	0.565884	75.85345	271.9074	−48	−26.7143	2	−7.53	−5.08714	1.1	−6.8	13.98286	21	14	2004–2006	Palermo (Italy), Central Mediterranean
Bweremana	1470	724496.5	9813727	9.866716	110.7962	218.1063	−12.22	10.84478	58.89	−3.42	−0.27187	5.981	−3.582	13.01974	20.2	23	2013–2015	Virunga (RD Congo), Central−Eastern Africa
Sake	1514	728715.6	9826678	4.258267	107.4899	206.474	−18.1	8.953478	41.74	−4.151	−0.80604	4.037	5.544	15.40183	19.69	23	2013–2015	Virunga (RD Congo), Central−Eastern Africa
Kingi	1848	730385.9	9835498	14.12498	139.4496	283.1228	−17.91	3.301111	29.46	−4.215	−1.61806	1.44	13.418	16.24556	19.198	18	2013–2015	Virunga (RD Congo), Central−Eastern Africa
Buhimba	1468	739267.8	9819303	5.712309	119.8702	223.6109	−21.47	7.099	37.44	−4.74	−1.1742	2.44	11.11	16.4926	20.49	20	2013–2015	Virunga (RD Congo), Central−Eastern Africa
OVG	1535	747783.8	9813927	7.270212	104.513	214.7828	−17.73	4.538571	32.87	−3.989	−1.37557	2.51	6.47	15.54314	20.37	21	2013–2015	Virunga (RD Congo), Central−Eastern Africa
Kanyaruchinya	1759	750928	9821494	7.477932	139.3237	320.3047	−18.47	8.913182	56.02	−4.604	−0.88568	6.16	6.74	15.99864	22.03	22	2013–2015	Virunga (RD Congo), Central−Eastern Africa
Kibati	1994	753477.1	9826430	5.400729	143.7377	263.8048	−23.7	5.287273	34.11	−4.869	−1.41464	1.856	11.24	16.60436	19.48	22	2013–2015	Virunga (RD Congo), Central−Eastern Africa
Rest 1	2254	752329.4	9828449	12.04778	194.1072	372.4425	−24.61	4.413571	46.8	−4.914	−1.62593	3.66	14.694	17.421	20.816	14	2013–2015	Virunga (RD Congo), Central−Eastern Africa

Table 1. *Cont.*

Site Name	Elevation (m a.s.l.)	UTM Coordinates		Precipitation (mm/month)			δ^2H (‰)			$\delta^{18}O$ (‰)			d−excess (‰)			Number of Samples	Sapling Periode	Region
		Easting	Northing	Min	Average	Max	Min	Average	Max	Min	Average	Max	Min	Average	Max			
Rest 2	2535	751531.9	9829124	15.3713	188.3133	376.597	−25.84	0.899286	41.5	−5.416	−2.18807	2.49	15.922	18.40386	21.58	14	2013–2015	Virunga (RD Congo), Central−Eastern Africa
Shaheru	2761	750846.7	9829631	53.1764	176.3632	339.2073	−27.27	2.9925	39.75	−5.657	−2.01108	2.53	17.41	19.08117	20.862	12	2013–2015	Virunga (RD Congo), Central−Eastern Africa
Biraro	2918	750760.4	9830145	35.7279	194.3483	357.279	−30.54	−2.02	34.51	−5.989	−2.75958	1.66	17.372	20.05667	21.834	12	2013–2015	Virunga (RD Congo), Central−Eastern Africa
Cabanes	3230	750386.9	9830663	47.9834	177.0123	338.9996	−32.3	−3.7275	29.08	−6.358	−3.01342	0.95	18.564	20.37983	23.476	12	2013–2015	Virunga (RD Congo), Central−Eastern Africa
Summit	3460	749852	9831197	23.26468	174.5993	274.3986	−32.53	−7.192	32.64	−6.435	−3.4971	1.28	18.74	20.7848	22.918	10	2013–2015	Virunga (RD Congo), Central−Eastern Africa

3.2. Spatiotemporal Variabilities of $\delta^{18}O$, $\delta^{2}H$ and D-Excess

As mentioned in Section 3.1, clearly defined seasonal variations are observed for both $\delta^{2}H$ and $\delta^{18}O$ in the two regions (Figure 3), with higher values found during the dry seasons in Virunga (July and August, and during the short dry season of mid-January to mid-February (Figure 3A,B) and during the summer months in the Central Mediterranean (Figure 3B,D). Conversely, the most depleted δ values were obtained during the rainy season in Virunga (principally from October to December and March to June) and during the cold and rainy winter period in the Central Mediterranean. In Virunga, samples from the lower altitudes generally showed the enriched $\delta^{2}H$ and $\delta^{18}O$ values during the sampling period; this is responsible for the alignment observed in the mean data points shown in the $\delta^{2}H$ versus $\delta^{18}O$ chart in Figure 2B. Similar behaviors were observed in $\delta^{2}H$ and $\delta^{18}O$ data collected from the Central Mediterranean.

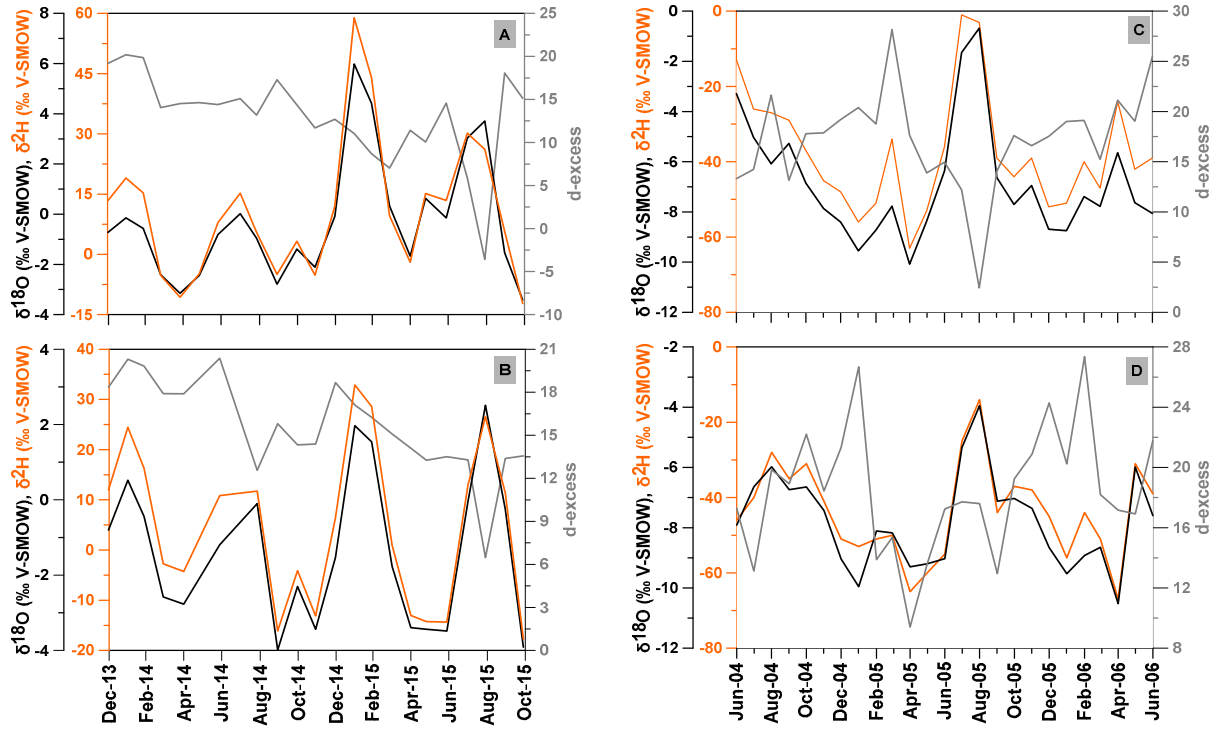

Figure 3. Temporal variation of $\delta^{2}H$, $\delta^{18}O$ and d-excess in monthly precipitation in Virunga (**A**,**B**), located on the limit between Central and Eastern Africa, within the western branch of the East African Rift System, and in the Central Mediterranean (**C**,**D**), Sicily in sourthern Italy.

Therefore, strong negative relationships were found between both the mean precipitation-weighted $\delta^{2}H$ and $\delta^{18}O$ and the altitude, while, conversely, the deuterium excess showed a strong positive relationship with the altitude (Figure 4). Virunga shows slightly higher vertical oxygen (−0.15‰/100 m) and hydrogen (−0.86‰/100 m) gradients compared to the Central Mediterranean area, where the vertical oxygen and hydrogen gradients are −0.24‰/100 m and −1.00‰/100 m for Stromboli and −0.16‰/100 m and −1.07‰/100 m for Sicily. However, Stromboli showed the higher d-excess gradient of 0.89/100 m (Virunga has a value of 0.32/100 m), which is consistent with the fact that the d-excess gradient has an opposite trend to that of the vertical oxygen and hydrogen gradients. The oxygen and hydrogen gradients for the Central Mediterranean area consistent with those previously reported for Sicily (e.g., [45–47]).

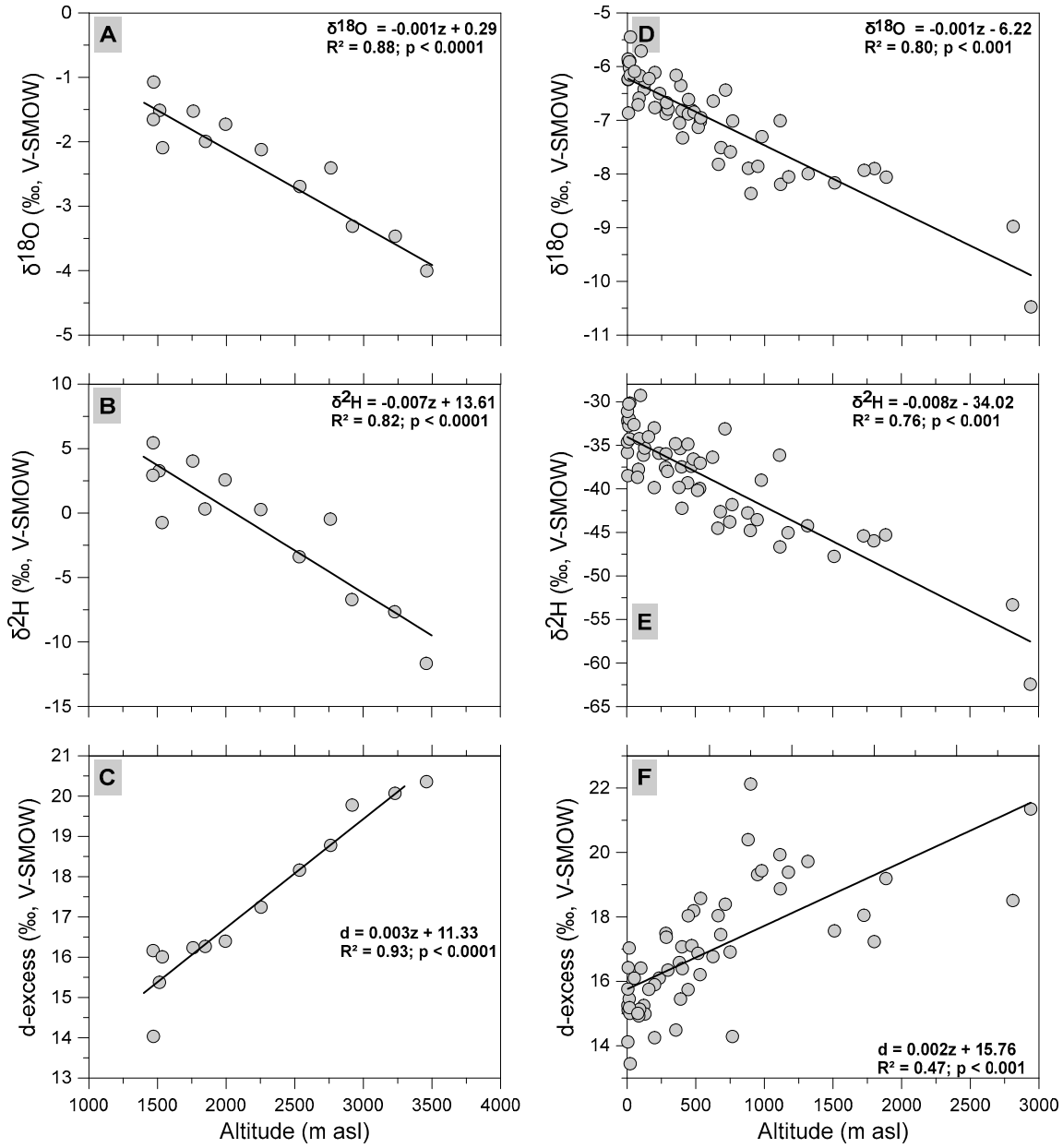

Figure 4. Mean precipitation-weighted δ^2H, $\delta^{18}O$ and d-excess values plotted against altitude in Virunga, (**A**–**C**) located on the limit between Central and Eastern Africa, within the western branch of the East African Rift System, and southern Italy (**D**–**F**) in the Central Mediterranean (data are from Stromboli and Sicily).

The high vertical oxygen and hydrogen gradients for Virunga are because of the high slope at Mt Nyiragongo, along which part of the samples were collected. Hence, in Virunga, a difference in gradients is observed between samples collected from the lowland sites found below 2000 m a.s.l. and those from the highland ones found above this altitude (see further discussions in [29,30]). Both the oxygen and hydrogen gradients at highland sites are 2-fold higher in comparison to those of lowland sites; these high values increase the overall gradient for Virunga. This difference is also attributed to two other important parameters: (1) different moistures affect highland and lowland areas in Virunga, and (2) the effect of precipitation amounts as they greatly vary between the low and highland sites (further discussed in Section 3.4). In the Central Mediterranean area, particularly in Stromboli Island, the local topography does not allow to us evaluate for such an effect.

3.3. Meteorological Effects: Temperature and Precipitation Amount

The Virunga monthly air temperature means are nearly constant for a given station, and therefore show variations generally less than 2 °C at an annual time scale (Figure 5A,B), because the region is located close to the equator. However, significant air temperature differences are observed between mean monthly values from stations found at different altitudes (e.g., compare temperature values of Figure 5A,B), or during diurnal air temperature variations at a given station. At a regional scale, in the Central and Eastern African regions nearing Virunga, precipitation is principally formed from the condensation of continental recycled moisture. The dominant evaporating and evapotranspiring surfaces are found in local lowlands [30,48–50], and hence the surface air temperature at moisture source regions is comparable to that of the study area. Such a lack of spatiotemporal variation in the air temperature results in the noticed lack of dependency between $\delta^{18}O$ and the air temperature in Virunga (Figure 5A,B), and is the common trend found in tropical regions [3,51,52].

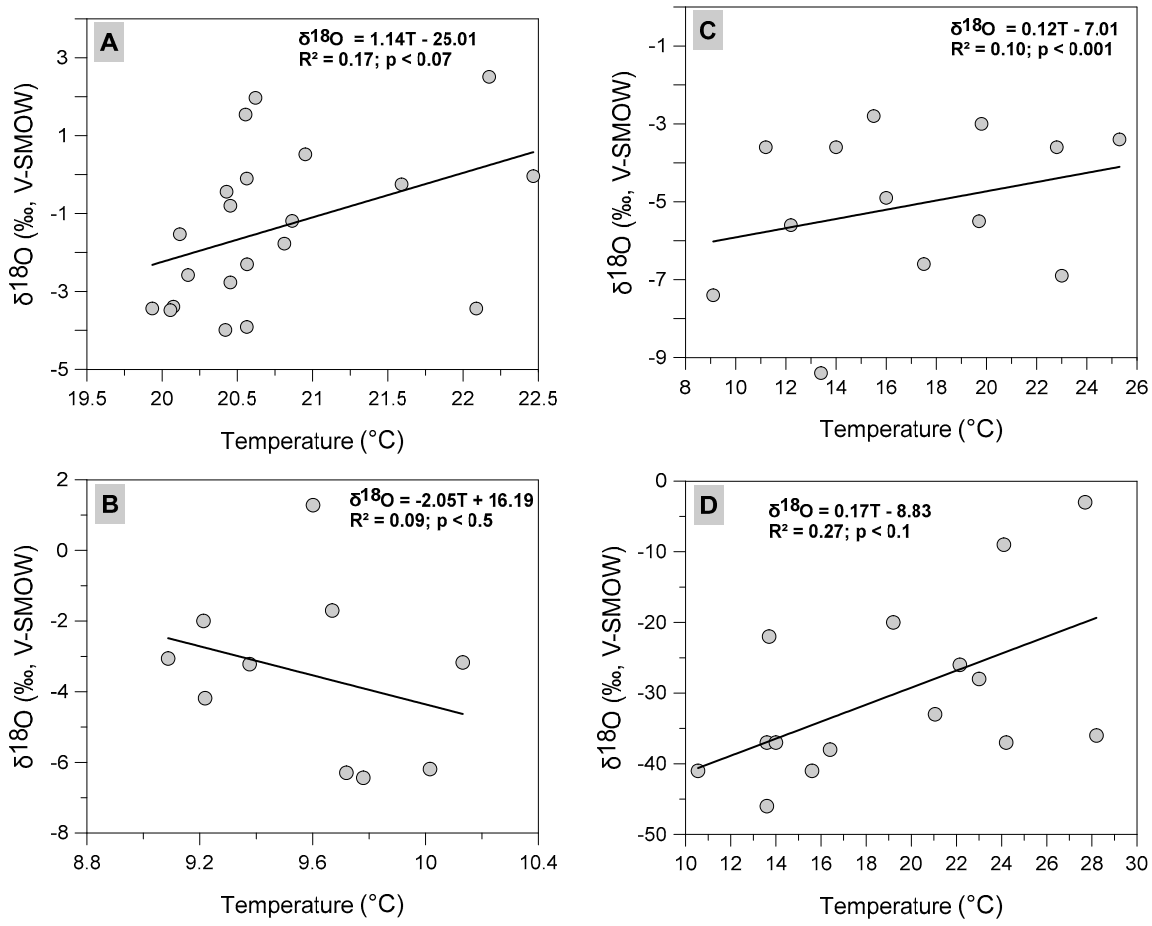

Figure 5. $\delta^{18}O$ monthly values from isolated stations plotted against temperature in Virunga, located on the limit between Central and Eastern Africa, within the western branch of the East African Rift System (**A**,**B**), and the Central Mediterranean (**C**,**D**). In Virunga, the data used in A and B are respectively from the OVG (1535 m a.s.l.) and summit (3460 m a.s.l.) stations (see map of Figure 1A), while in the Central Mediterranean the data used in C are from a station in the Spagnuola area (see map of Figure 1B2) and data for D are from the LBR station in Stromboli (see map of Figure 1B1). No clear relationships can be recognized between isotope composition and temperature.

Virunga monthly $\delta^{18}O$, $\delta^{2}H$ and d-excess show weak correlation with monthly precipitation amounts (R^2 varies from 0.11 to 0.32 for $\delta^{18}O$; 0.13 to 0.34 for $\delta^{2}H$ and 0.00 to 0.45 for d-excess). Particularly, the $\delta^{18}O$ dependency averages 2.96 ‰/100 mm of monthly precipitation, but ranges from 2.10 to 4.51 ‰/100 mm. A combination of monthly precipitation amounts, and the altitudes show

that the $\delta^{18}O$ precipitation amounts dependency is higher in lowlands, which was likely favored by the influence from the heavier water vapor from the neighboring Lake Kivu [30]. The $\delta^{18}O$, $\delta^{2}H$ and d-excess relationships with monthly precipitation amounts show higher correlations when mean precipitation-weighted and the average annual precipitation values are plotted, and give an R^2 of 0.58 for $\delta^{18}O$ (Figure 6A), 0.49 for $\delta^{2}H$ (Figure 6B) and 0.76 for d-excess (Figure 6C).

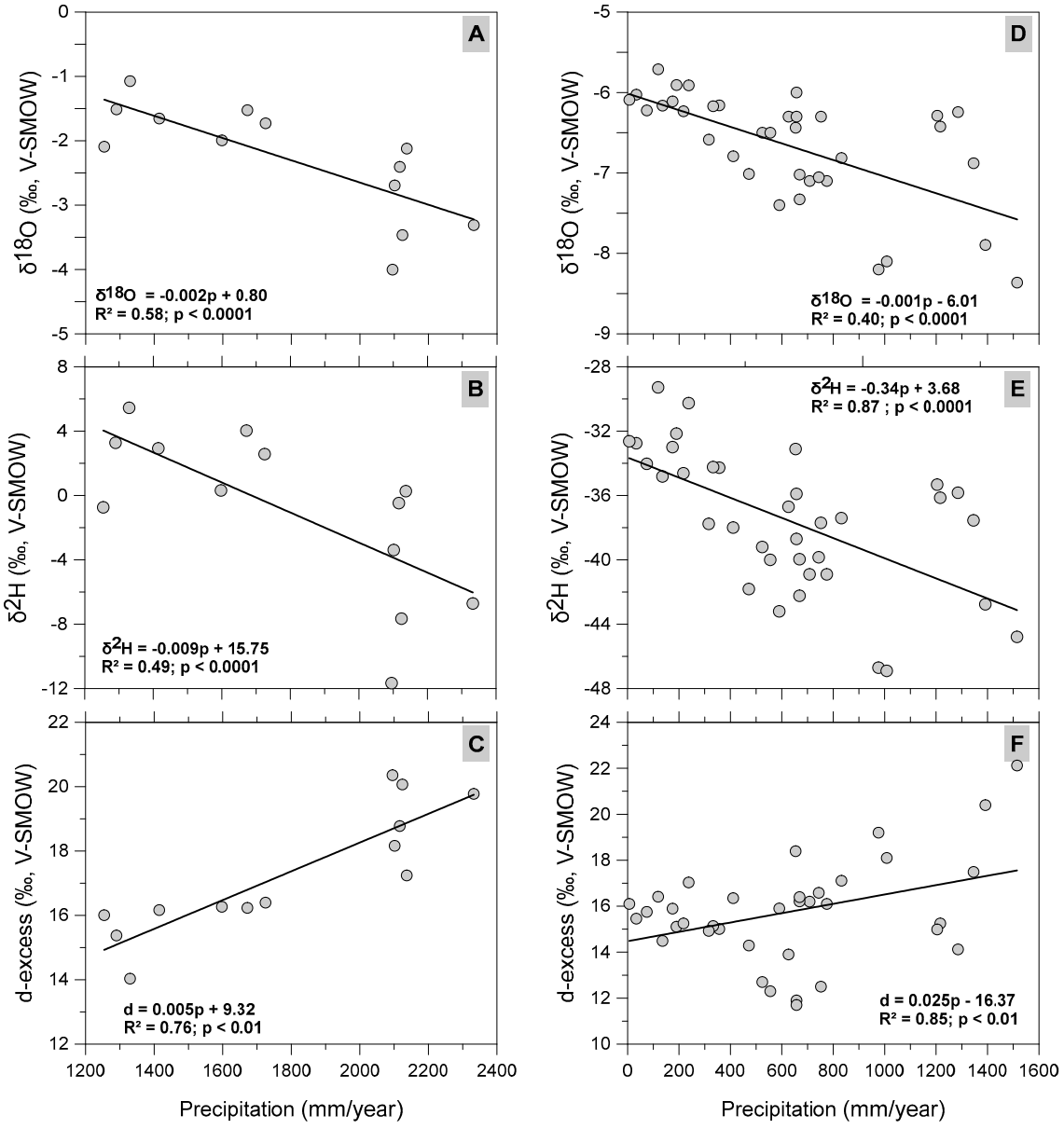

Figure 6. Mean precipitation-weighted $\delta^{18}O$, $\delta^{2}H$ and d-excess values plotted against averaged annual precipitation in Virunga, located on the limit between Central and Eastern Africa, within the western branch of the East African Rift System (**A**–**C**), and southern Italy (**D**–**F**) in the Central Mediterranean (data are from Stromboli and Sicily). The two areas exhibit a different extent in the negative correlation between the isotope composition against the precipitation amount (**A**,**B**,**D**,**E**), and in the positive correlation between deuterium excess against the precipitation amount (**C**,**F**).

In the Central Mediterranean, monthly air temperature averages show a clear seasonality with the lower values in winter and high values in summer (Figure 6C,D). In addition, significant air temperature differences are observed between mean monthly values from stations at different altitudes with diurnal air temperature variations. The Central Mediterranean monthly $\delta^{18}O$, $\delta^{2}H$ and d-excess

show weak correlation with monthly precipitation amounts. The $\delta^{18}O$, $\delta^{2}H$ and d-excess relationships with precipitation amounts show higher correlations when mean precipitation-weighted and the average annual precipitation values are plotted, and give anR^2 of 0.40, 0.87 and 0.85 for $\delta^{18}O$, $\delta^{2}H$ and d-excess, respectively.

3.4. Precipitation Stable Isotope Fractionation in Virunga and in the Central Mediterranean

3.4.1. Stable Isotope Fractionation in Virunga

Virunga LMWL has a higher intercept compared to the GMWL, and it shows a slope comparable to that of the GMWL (Figure 2A) and that from other Central African regions (e.g., [12,53–55]. Such a slope suggests processes of rain formation under equilibrium conditions at the regional scale. In addition, the intercept indicates that Virunga precipitation originates from high-altitude recycled continental moisture [15,56]. The high d-excess values of precipitation are the consequence of vapor formation under non-equilibrium conditions at source, favored by both low RH and strong winds. A difference of ~10‰ in the d-excess values is observed when comparing lowland to highland areas of Virunga, and is caused by the kinetic fractionation during vapor formation and moisture transportation, and by the difference in the composition of the moistures arriving in the low and highlands.

A secondary process additionally affects the raindrops during their fall as they pass through the water vapor in the lower atmosphere [30]. In fact, the pristine falling raindrops interact with the isotopically-enriched water vapor present in the lower atmosphere, the vapor coming mostly from Lake Kivu. This lake has isotopically enriched surface waters, showing values up to 27.76‰ and 3.68‰ for $\delta^{2}H$ and $\delta^{18}O$, respectively [30]. The lower atmosphere in the study area is, thus, saturated in isotopically enriched water vapor when considering the recorded high RH (monthly values range: ~70 to 90%). According to [57], such high RH favors equilibrium between the falling raindrops and the water vapor, a process that likely contributes to the $\delta^{2}H$ and $\delta^{18}O$ enrichment of Virunga lowland precipitation. Therefore, Virunga highlands receive only precipitation from the upper atmosphere produced from remote moisture sources, whereas the lowland areas are additionally affected by local water vapor that mediates the enrichment of the falling raindrops.

The moisture source regions for Virunga abound in small to large open surface waters, the surface waters of the lakes are particularly isotopically enriched (e.g., [30,58–65]). The enrichment of their surface waters in the heavy isotopes is due to the intense evaporation process that in some cases exceeds the precipitation they receive over their surfaces. These lakes represent the predominant source of water vapor for the atmosphere during the dry periods, while during the rainy season the soil/plants evapotranspiration is the major source (further discussed in [30]). Because the plants-transpired vapor tends to be isotopically similar to the liquid water drawn into its roots (e.g., [66,67]), there are few variations in the $\delta^{2}H$ and $\delta^{18}O$ during the rainy season when considering the abundant neighboring tropical forest and other isolated plants. Thus, the precipitation from the rainy season is isotopically depleted because it is derived from the condensation of vapor from (1) freshly precipitated rain, (2) plants-transpired vapor and (3) because of the high precipitation amount. Conversely, during the dry season, the residual soil-water that is then evaporating will be composed of heavier isotopes, and this vapor mixes with the permanently enriched vapor from the lakes and, thus, yields enriched precipitation.

The changes in wind direction also influence the precipitation $\delta^{2}H$ and $\delta^{18}O$, as it brings moisture from different sources. In fact, the equatorial East African region experiences three major air streams: the northeast monsoon system, the southeast monsoon system from the Indian Ocean, and the southwesterly humid air from the Congo basin [68]. The NE, E and SE winds bring moisture evaporated from Lake Edward, Lake Albert and Lake Victoria surface waters, in addition to that evapotranspired in their moderately to densely forested catchments. Conversely, the S and SW winds carry moisture evapotranspired in the Tanganyika-Kivu basins, especially that from the neighboring Lake Kivu. Once in the study area, the NE, E and SE winds principally occupy the upper atmosphere

as they originate from outside the rift, while the S and SW follow the low-lying channel of the rift and are consequently maintained in the lower atmosphere. Thus, the NE and E originating high-speed air mass moves upward as a result of topography changes and might yield orographic lifting at Virunga Mountains. The moisture they bring principally influences the δ^2H and $\delta^{18}O$ of the precipitation of highland sites, whereas the S and SW low-level moisture additionally influences that of lowland sites. The high speeds of the NE and E-SE winds yield the earlier discussed kinetic fractionation that lead to the higher d-excess values that characterize the precipitation of highland sites. Conversely, the S and SW winds in the lower atmosphere are less strong and favor a relatively equilibrium fractionation in conjunction with the high RH prevalent in lowland areas. Because of the topographic constraints of the rift structure and the prevailing weak winds, this S to SW originating moisture is essentially permanent in the lower atmosphere and drives the earlier noted isotopic enrichment of the falling rain drops.

3.4.2. Stable Isotope Fractionation in the Central Mediterranean

At a regional scale, in the Central Mediterranean, precipitation is principally formed from the condensation maritime vapor forming over the Atlantic Ocean as well as from the Mediterranean Sea [32,33]. The Mediterranean Sea is a classic example of a reservoir producing water vapor characterized by high deuterium excess [13,16]. Such an effect depends on kinetic fractionation occurring when dry air masses travel over the sea surface. This effect coupled with the kinetic condensation of local orographic clouds, forming on significant topographic features such as hills and mountains, is responsible for the high deuterium excess found in rain samples from mountains in the Central Mediterranean. The high seasonal variation in d-excess between summer and winter reflects the climatic features and circulation patterns of the Central Mediterranean. In fact, when cold air masses, characterized by low relative humidity, travel over seawater, kinetic fractionation produces high deuterium excess values in the vapor, whereas the movement of warm air masses, usually characterized by high relative humidity, leads to lower deuterium excess values [33]. At Stromboli Island, the production of volcanic aerosol close to the craters favors the non-equilibrium condensation of water droplets. Under these conditions, the diffusional growth of hydrometeors could cause a great deuterium excess as a result of the higher diffusivity of $HD^{16}O$ compared to that of $H_2{}^{18}O$ [69]. Therefore, the coalescence of raindrops and haze droplets in the orographic cloud generates the increase in the deuterium excess values in the rain. Consequently, the composition of the precipitation is not changed directly by volcanic activity. Nevertheless, the production of volcanic aerosols could indirectly enhance deuterium excess in rain near the craters.

4. Conclusions

Virunga precipitation originates from high-altitude recycled continental moisture. The slope of the LMWL further reveals that during the condensation, rainwater forms under equilibrium, conditions as is the case for central Africa forest regions, whereas the higher intercept and the $\delta^{18}O$ values are closer to those from the East Africa region. Even though Virunga is generally a high-altitude region, a clear shift is observed between the isotope composition of the precipitation from the local lowland and highland sites, which is topographically driven. In fact, the lowland sites are characterized by higher δ^2H and $\delta^{18}O$ and lower d-excess values, while the highland areas have lower δ^2H and $\delta^{18}O$ and higher d-excess. The values δ^2H, $\delta^{18}O$ and d-excess at low- and highland areas are in line with the weather patterns such as the temperature (temperature is lower at highland and higher at lowland areas), wind speed and direction (high speed and of well-defined direction at highland, calm and generally lacking of unique-direction at lowland) or precipitation (higher and lower precipitation at highland and lowland areas, respectively). The monthly δ^2H and $\delta^{18}O$ showed a well-defined seasonality, with the heavier δ^2H and $\delta^{18}O$ obtained during the dry periods and the lighter, in the wet periods, with strong correlation to precipitation amount. The vapor from the East African Great Lakes has a strong influence on the isotopic composition of Virunga precipitation, particularly during the dry season, while in the rainy season, the precipitation is mainly formed from soil/plants evapotranspiration. No

$\delta^{18}O$ dependency on air temperature was observed as is generally the case for tropical regions, while the $\delta^{18}O$ and $\delta^{2}H$ are negatively correlated to precipitation amounts.

In the Central Mediterranean, the isotopic composition of precipitation clearly reflects the origin of the vapor feeding the raindrops. The climatic and morphological features of the Mediterranean represent a unique natural environment where air masses, mainly coming from the Atlantic Ocean, travel over the Mediterranean Sea and produce rain events from the condensation of water with different proportions of vapor from different areas. In addition, local orographic clouds induce a kinetic condensation process. With respect to Virunga, precipitation occurring in the Central Mediterranean does not show any clear contribution from the re-evaporated air masses, because of the poor vegetation cover and the regional air circulation systems.

The marked differences of the isotopic composition of precipitation in Virunga and in the Central Mediterranean reflect very different climatic and morphological features, where several fractionation processes and vapor sources play dissimilar roles. This study, thus, represents a key paper for researchers dealing with this topic.

Author Contributions: C.M.B. and M.L. drafted the manuscript, which they had latter amended and approved.

Funding: This research received no external funding and "the APC was funded by the Istituto Nazionale di Geofisica e Vulcanolgia - Sezione di Palermo.

Acknowledgments: Virunga water samples were analyzed in the isotope hydrology laboratory of the International Atomic Energy Agency (IAEA) within the framework of the Global Network of Isotopes in Precipitation. A few other samples from Virunga were analyzed at INGV-Palermo, where all the samples from Sicily and Stromboli were analyzed. The authors acknowledge insightful comments from Wendy McCausland (U.S. Geological Survey), and comments and recommendations from two anonymous reviewers who improved the manuscript; and the editorial handling of Autumn Du.

Conflicts of Interest: The authors declare no conflict of interest.

References

1. Kendall, C.; Caldwell, E.A. Fundamentals of Isotope Geochemistry. In *Isotope Tracers in Catchment Hydrology*; Kendall, C., McDonnell, J.J., Eds.; Elsevier Science: Amsterdam, The Netherland, 1998; pp. 51–86.
2. *Environmental Isotopes in the Hydrological Cycle, Principles and Applications, Vol. 1*; Mook, W.G. (Ed.) IAEA/UNESCO: Paris, France; Vienna, Austria, 2000.
3. Gat, J.R.; Mook, W.G.; Meijer, H.A. *Environmental Isotopes in the Hydrological Cycle, Principles and Applications, Vol. 2: Atmospheric Water*; UNESCO/IAEA Series; IAEA/UNESCO: Paris, France; Vienna, Austria, 2001.
4. Hoefs, J. *Stable Isotope Geochemistry*, 6th ed.; Springer: Berlin/Heidelberg, Germany, 2009; 293p. [CrossRef]
5. Gat, J.R. *Isotope Hydrology: A Study of the Water Cycle*; Imperial College Press: London, UK, 2010; 197p.
6. Craig, H. Isotopic variations in meteoric waters. *Science* **1961**, *133*, 1702–1703. [CrossRef] [PubMed]
7. Gonfiantini, R. Standards for stable isotope measurements in natural compounds. *Nature* **1978**, *271*, 534–536. [CrossRef]
8. Dansgaard, W. Stable isotopes in precipitation. *Tellus* **1964**, *16*, 438–468. [CrossRef]
9. Craig, H.; Gordon, L. Deuterium and oxygen-18 variations in the ocean and marine atmosphere. In *Stable Isotopes in Oceanographic Studies and Paleotemperatures*; Tongiorgi, E., Ed.; Consiglio Nazionale delle Richerche, Laboratorio de Geologia Nucleare: Pisa, Italy, 1965.
10. Ehhalt, D.; Knott, K.; Nagel, J.F.; Vogel, J.C. Deuterium and oxygen-I 8 in rain water. *J. Geophys. Res.* **1963**, *68*, 3775–3780. [CrossRef]
11. Yurtsever, Y. *World Survey of Stable Isotopes in Precipitation*; IAEA Internal Report; IAEA: Vienna, Austria, 1975.
12. Gonfiantini, R.; Roche, M.A.; Olivry, J.C.; Fontes, J.C.; Zuppi, G.M. The altitude effect on the isotopic composition of tropical rains. *Chem. Geol.* **2001**, *181*, 147–167. [CrossRef]
13. Gat, J.R.; Carmi, I. Evolution of the isotopic composition of atmospheric waters in the Mediterranean Sea area. *J. Geophys. Res.* **1970**, *75*, 3039–3048. [CrossRef]
14. Merlivat, L.; Jouzel, J. Global climatic interpretation of the deuterium-oxygen 18 relationship for precipitation. *J. Geophys. Res.* **1979**, *84*, 5029–5033. [CrossRef]

15. Froehlich, K.; Gibson, J.J.; Aggarwal, P.K. Deuterium excess in precipitation and its climatological significance. In *Study of Environmental Change Using Isotope Techniques*; International Atomic Energy Agency: Vienna, Austria, 2002; pp. 54–65.
16. Gat, J.R.; Klein, B.; Kushnir, Y.; Roether, W.; Wernli, H.; Yam, R.; Shemesh, A. Isotope composition of air moisture over the Mediterranean Sea: An index of the air–sea Interaction pattern. *Tellus* **2003**, *55B*, 953–965. [CrossRef]
17. Dansgaard, W.; Johnsen, S.; Møller, J.; Langway, C., Jr. One thousand centuries of climatic record from Camp Century on the Greenland ice sheet. *Science (New York, NY)* **1969**, *166*, 377. [CrossRef]
18. Fisher, D.A. Remarks on the deuterium excess in precipitation in cold regions. *Tellus* **1991**, *43B*, 401–407. [CrossRef]
19. Augustin, L.; EPICA Community Members. Eight glacial cycles from an Antarctic ice core. *Nature* **2004**, *429*, 623–628. [CrossRef] [PubMed]
20. Hanna, E. *Surface Temperature Reconstructions for the Last 2000 Years*; The National Academies Press: Washington, DC, USA, 2006; ISBN 0 30 9102 251.
21. Werner, M.; Jouzel, J.; Masson-Delmotte, V.; Lohmann, G. Reconciling glacial Antarctic water stable isotopes with ice sheet topography and the isotopic paleothermometer. *Nature* **2018**, *9*, 3537. [CrossRef] [PubMed]
22. Balagizi, M.C.; Darchambeau, F.; Yalire, M.M.; Bouillon, S.; Borges, V.A. River geochemistry, chemical weathering, and atmospheric CO_2 consumption rates in the Virunga Volcanic Province (East Africa). *Geochem. Geophys. Geosyst.* **2015**, *16*, 2637–2660. [CrossRef]
23. Cuoco, E.; Tedesco, D.; Poreda, R.J.; Williams, J.C.; De Francesco, S.; Balagizi, M.C.; Darrah, T.H. Impact of volcanic plume emissions on rain water chemistry during the January 2010 Nyamulagira eruptive event: Implications for essential potable water resources. *J. Hazard. Mater.* **2012**, *244*, 570–584. [CrossRef] [PubMed]
24. Cuoco, E.; Spagnuolo, A.; Balagizi, M.C.; De Francesco, S.; Tassi, F.; Vaselli, O.; Tedesco, D. Impact of volcanic emissions on rainwater chemistry: The case of Mt. Nyiragongo in the Virunga volcanic region (DRC). *J. Geochem. Explor.* **2012**, *125*, 69–79. [CrossRef]
25. Coppola, D.; Campion, R.; Laiolo, M.; Cuoco, E.; Balagizi, M.C.; Ripepe, M.; Cigolini, C.; Tedesco, D. Birth of a lava lake: Nyamulagira volcano 2012–2015. *Bull. Volcanol.* **2016**, *78*, 20. [CrossRef]
26. Bobrowski, N.; Giuffrida, G.B.; Yalire, M.; Lübcke, P.; Arellano, S.; Balagizi, C.; Calabrese, S.; Galle, B.; Tedesco, D. Multi-component gas emission measurements of the active lava lake of Nyiragongo, DR Congo. *J. Afr. Earth Sci.* **2016**, *134*, 856–865. [CrossRef]
27. Balagizi, M.C.; Yalire, M.M.; Ciraba, M.H.; Vicky, B.K.; Minani, S.A.; Kinja, K.A. Kasereka $MMCO_2$ and SO_2 emissions, temperature variations and field observations before and after the February 29, 2016 new vent inside Nyiragongo crater. *Bull. Volcanol.* **2016**, *78*, 64. [CrossRef]
28. Balagizi, M.C.; Kies, A.; Kasereka, M.M.; Tedesco, D.; Yalire, M.M.; McCausland, W.A. Natural hazards in Goma and the surrounding villages, East African Rift System. *Nat. Hazards* **2018**, *93*, 31–66. [CrossRef]
29. Balagizi, M.C.; Kasereka, M.M.; Cuoco, E.; Liotta, M. Rain-plume interactions at Nyiragongo and Nyamulagira volcanoes and associated rainwater hazards, East Africa. *Appl. Geochem.* **2017**, *81*, 76–89. [CrossRef]
30. Balagizi, M.C.; Kasereka, M.M.; Cuoco, E.; Liotta, M. Influence of moisture source dynamics and weather patterns on stable isotopes ratios of precipitation in Central-Eastern Africa. *Sci. Total Environ.* **2018**, *628*, 1058–1078. [CrossRef] [PubMed]
31. Catalano, R.; Di Stefano, P.; Sulli, A.; Vitale, F.P. Paleogeography and structure of the central Mediterranean: Sicily and its offshore area. *Tectonophysics* **1996**, *260*, 291–323. [CrossRef]
32. Liotta, M.; Brusca, L.; Grassa, F.; Inguaggiato, S.; Longo, M.; Madonia, P. Geochemistry of rainfall at Stromboli volcano (Aeolian Islands): Isotopic composition and plume–rain interaction. *Geochem. Geophys. Geosyst.* **2006**, *7*. [CrossRef]
33. Liotta, M.; Favara, R.; Valenza, M. Isotopic composition of the precipitations in the central Mediterranean: Origin marks and orographic precipitation effects. *J. Geophys. Res.* **2006**, *111*. [CrossRef]
34. Bolle, H.-J. *Mediterranean Climate: Variability and Trends*; Springer: Berlin, Germany, 2003.
35. Buzzi, A.; Tibaldi, S. Cyclogenesis in the lee of the Alps- a case study. *Q. J. R. Meteorol. Soc.* **1978**, *104*, 271–287. [CrossRef]
36. Buzzi, U.H.; Stergiou, N.; Kurz, M.J.; Hageman, P.A.; Heidel, J. Nonlinear dynamics indicates aging affects variability during gait. *Clin. Biomech.* **2003**, *18*, 435–443. [CrossRef]

37. Lionello, P.; Sanna, A. Mediterranean wave climate variability and its links with NAO and Indian Monsoon. *Clim. Dyn.* **2006**, *25*, 611–623. [CrossRef]
38. Chaboureau, J.-P.; Claud, C. Satellite-based climatology of Mediterranean cloud systems and their association with large-scale circulation. *J. Geophys. Res.* **2006**, *111*, D01102. [CrossRef]
39. Gaertner, M.A.; Jacob, D.; Gil, V.; Domínguez, M.; Padorno, E.; Sánchez, E.; Castro, M. Tropical cyclones over the Mediterranean Sea in climate change simulations. *Geophys. Res. Lett.* **2007**, *34*, L14711. [CrossRef]
40. Mariotti, A.; Struglia, M.V.; Zeng, N.; Lau, K.M. The hydrological cycle in the Mediterranean region and implications for the water budget of the Mediterranean Sea. *J. Clim.* **2002**, *15*, 1674–1690. [CrossRef]
41. Liotta, M.; Bellissimo, S.; Favara, R.; Valenza, M. Isotopic composition of single rain events in the central Mediterranean. *J. Geophys. Res.* **2008**, *113*, D16304. [CrossRef]
42. Liotta, M.; Grassa, F.; D'Alessandro, W.; Favara, R.; Gagliano Candela, E.; Pisciotta, A.; Scaletta, C. Isotopic composition of precipitation and groundwater in Sicily, Italy. *Appl. Geochem.* **2013**, *34*, 199–206. [CrossRef]
43. Wassenaar, L.I.; Coplen, T.B.; Pradeep, K.A. Approaches for achieving long-term accuracy and precision of δ18O and δ2H for waters analyzed using laser absorption spectrometers. *Sci. Technol.* **2014**, *48*, 1123–1131. [CrossRef] [PubMed]
44. Coplen, T.B.; Wildman, J.D.; Chen, J. Improvements in the gaseous hydrogen-water equilibration technique for hydrogen isotope-ratio analysis. *Anal. Chem.* **1991**, *63*, 910–912. [CrossRef]
45. Hauser, S.; Dongarra, G.; Favara, R.; Longinelli, A. Composizione isotopica delle pioggie in Sicilia. Riferimenti di base per studi idrogeologici e relazione con altre aree mediterranee. *Rend. Soc. Ital. Miner. Pet.* **1980**, *36*, 671–680.
46. Favara, R.; Grassa, F.; Ingaggiato, S.; D'Amore, F. Geochemical and hydrogeological characterization of thermal springs in western Sicily, Italy. *J. Volcanol. Geotherm. Res.* **1998**, *84*, 125–141. [CrossRef]
47. Poage, M.A.; Chamberlain, C.P. Empirical relationships between elevation and the stable isotope composition of precipitation and surface waters: Considerations for studies of paleoelevation change. *Am. J. Sci.* **2001**, *301*, 1–15. [CrossRef]
48. Zomer, R.J.; Bossio, D.A.; Trabucco, A.; Yuanjie, L.; Gupta, D.C.; Singh, V.P. *Trees and Water: Smallholder Agroforestry on Irrigated Lands in Northern India*; IWMI Research Report 122; International Water Management Institute: Colombo, Sri Lanka, 2007; p. 45.
49. Zomer, R.J.; Trabucco, A.; Bossio, D.A.; van Straaten, O.; Verchot, L.V. Climate Change Mitigation: A Spatial Analysis of Global Land Suitability for Clean Development Mechanism Afforestation and Reforestation. *Agric. Ecosyst. Environ.* **2008**, *126*, 67–80. [CrossRef]
50. Trabucco, A.; Zomer, R.J. Global Aridity Index (Global-Aridity) and Global Potential Evapotranspiration (Global-PET) Geospatial Database. CGIAR Consortium for Spatial Information. 2009. Available online: http://www.csi.cgiar.org (accessed on 25 July 2019).
51. Rozanski, K.; Araguaś-Araguaś, L.; Gonfiantini, R. Isotopic patterns inmodern global precipitation. In *Climate Change in Continental Isotopic Records*; Swart, P.K., Lohmann, K.C., Mckenzie, J., Savin, S., Eds.; American Geophysical Union: Washington, DC, USA, 1993; Volume 78, pp. 1–35. [CrossRef]
52. Bowen, G. Spatial analysis of the intra-annual variation of precipitation isotope ratios and its climatological corollaries. *J. Geophys. Res.* **2008**, *113*, D05113. [CrossRef]
53. Fontes, J.C.; Olivry, J.C. *Gradient Isotopique Entre 0 et 4000 m Dans les Précipitations du Mont Cameroun*; Quatrième. Réunion Annuelle des Sciences de la Terre, Société Géologique de France.: Paris, France, 1976.
54. Munyaneza, O.; Wenninger, J.; Uhlenbrook, S. Identification of runoff generation processes using hydrometric and tracer methods in a meso-scale catchment in Rwanda. *Hydrol. Earth Syst. Sci.* **2012**, *16*, 1991–2004. [CrossRef]
55. Wirmvem, M.J.; Ohba, T.; Kamtchueng, B.T.; Taylor, E.T.; Fantong, W.Y.; Ako, A.A. Variation in stable isotope ratios of monthly rainfall in the Douala and Yaounde cities, Cameroon: Local meteoric lines and relationship to regional precipitation cycle. *Appl. Water Sci.* **2016**, 1–14. [CrossRef]
56. Pfahl, S.; Sodemann, H. What controls deuterium excess in global precipitation? *Clim. Past* **2014**, *10*, 771–781. [CrossRef]
57. Stewart, M.K. Stable isotope fractionation due to evaporation and isotopic-exchange of falling water drops: Applications to atmospheric processes and evaporation of lakes. *J. Geophys. Res.* **1975**, *80*, 1133–1146. [CrossRef]

58. Craig, H. *Lake Tanganyika Geochemical and Hydrographic Study: 1973 Expedition*; Report 75-5; Scripps Institute of Oceanography: La Jolla, CA, USA, 1975; 83p.
59. Gonfiantini, R.; Zuppi, G.M.; Eccles, D.H.; Ferro, W. Isotope investigation of Lake Malawi. In Proceedings of the International Symposium International Atomic Energy Agency, Vienna, Austria, 14–18 May 1979.
60. Cerling, T.E.; Bowman, J.R.; O'Neil, J.R. An isotopic study of a fluvial lacustrine sequence: The Plio-Pleistocene Koobi Fora sequence, East Africa. *Palaeogeogr. Palaeoclimatol. Palaeoecol.* **1988**, *63*, 335–356. [CrossRef]
61. Odada, E. Stable isotopic composition of East African lake waters. In *Use of Isotope Techniques in Lake Dynamics Investigations*; Gourcy, L., Ed.; IAEA: Vienna, Austria, 2001; pp. 43–48.
62. Bahati, G.; Pang, Z.; Armannsson, H.; Isabirye, E.M.; Kato, V. Hydrology and reservoir characteristics of three geothermal systems in Western Uganda. *Geothermics* **2005**, *34*, 568–591. [CrossRef]
63. Cockerton, H.E.; Street-Perrott, F.A.; Leng, M.J.; Barker, P.A.; Horstwood, M.S.A.; Pashley, V. Stable-isotope (H, O, and Si) evidence for seasonal variations in hydrology and Si cycling from modern waters in the Nile Basin: Implications for interpreting the Quaternary record. *Quat. Sci. Rev.* **2013**, *66*, 4–21. [CrossRef]
64. Jasechko, S.; Sharp, Z.D.; Gibson, J.J.; Birks, S.J.; Yi, Y.; Fawcett, P.J. Terrestrial water fluxes dominated by transpiration. *Nature* **2013**, *496*, 347–350. [CrossRef] [PubMed]
65. Balagizi, M.C.; Kasereka, M.M.; Terzer, S.; Cuoco, E.; Liotta, M. *Identifying Hydrological Pathways in the North Basin of Lake Kivu Using Stable Isotope Ratios of Meteoric Recharge and Surface Water*; Geophysical Research Abstracts Vol. 18, EGU2016-9720-1; EGU General Assembly: Vienna, Austria, 2016.
66. Harwood, K.G.; Gillon, J.S.; Griffiths, H.; Broadmeadow, M.S.J. Diurnal variation of $D^{13}CO_2$, $D.C.^{18}O^{16}O$ and evaporative site enrichment of $dH_2{}^{18}O$ in Piper aduncum under field conditions in Trinidad. *Plant Cell Environ.* **1998**, *21*, 269–283. [CrossRef]
67. Wang, L.; Good, S.; Caylor, K.; Cernusak, L.A. Direct quantification of leaf transpiration isotopic composition. *Agric. For. Meteorol.* **2012**, *154*, 127–135. [CrossRef]
68. Nicholson, S.E. A review of climate dynamics and climate variability in eastern Africa. In *The Limnology, Climatology and Paleoclimatology of the East African Lakes*; Johnson, T.C., Odada, E.O., Eds.; Gordon and Breach: Amsterdam, The Netherland, 1996; pp. 25–56.
69. Cappa, C.D.; Hendricks, M.B.; De Paolo, D.J.; Cohen, R.C. Isotopic fractionation of water during evaporation. *J. Geophys. Res.* **2003**, *108*, 4525. [CrossRef]